doi:10.1016/j.jmb.2005.11.019 J. Mol. Biol. (2006) 356, 111–120

JMB

Available online at www.sciencedirect.com

SCIENCE DIRECT®

ELSEVIER

# Crystal Structures of Protein Phosphatase-1 Bound to Motuporin and Dihydromicrocystin-LA: Elucidation of the Mechanism of Enzyme Inhibition by Cyanobacterial Toxins

**Jason T. Maynes[1], Hue A. Luu[1], Maia M. Cherney[1], Raymond J. Andersen[2] David Williams[2], Charles F. B. Holmes[1]* and Michael N. G. James[1]**

[1]*Canadian Institutes of Health Research, Group in Protein Structure and Function Department of Biochemistry Faculty of Medicine, University of Alberta, Edmonton, Alta Canada T6G 2H7*

[2]*Department of Chemistry University of British Columbia Vancouver, BC, Canada*

**Corresponding author*

The microcystins and nodularins are tumour promoting hepatotoxins that are responsible for global adverse human health effects and wildlife fatalities in countries where drinking water supplies contain cyanobacteria. The toxins function by inhibiting broad specificity Ser/Thr protein phosphatases in the host cells, thereby disrupting signal transduction pathways. A previous crystal structure of a microcystin bound to the catalytic subunit of protein phosphatase-1 (PP-1c) showed distinct changes in the active site region when compared with protein phosphatase-1 structures bound to other toxins. We have elucidated the crystal structures of the cyanotoxins, motuporin (nodularin-V) and dihydromicrocystin-LA bound to human protein phosphatase-1c (γ isoform). The atomic structures of these complexes reveal the structural basis for inhibition of protein phosphatases by these toxins. Comparisons of the structures of the cyanobacterial toxin:phosphatase complexes explain the biochemical mechanism by which microcystins but not nodularins permanently modify their protein phosphatase targets by covalent addition to an active site cysteine residue.



*Keywords:* crystal structure; cyanobacteria; microcystin; nodularin

## Introduction

Microcystin and nodularin (cyclic peptide hepatotoxins) are cyanobacterial metabolites found worldwide both in freshwater and in marine environments.[1] These toxins are responsible for wildlife fatalities and adverse human health effects in countries where drinking water supplies contain toxic cyanobacteria. The nodularins and microcystins are powerful liver tumour promoters and potent inhibitors of the protein phosphatase-1 and -2A catalytic subunits (PP-1c/PP-2Ac).[2–6] Inhibition of these enzymes in the liver has been associated with hepatocyte deformation due to reorganization of microfilaments.[7] Liver tumour promotion may be linked to the ability of these toxins to promote cytokeratin hyperphosphorylation associated with morphological changes in rat hepatocytes.[8]

Most heptapeptide microcystins differ in the nature of two variable L-amino acids and the absence of methyl groups on D-erythro-β-methyl aspartic acid (Masp) and/or *N*-methyldehydroalanine (Nmda) residues (Figure 1(a)).[9,10] Nodularins are structurally related cyclic pentapeptides that inhibit PP-1c/PP-2Ac with similar potency to that of the microcystins but only contain one variable amino acid site.[11] The hydrophobic pentapeptide motuporin (MOT, a member of the nodularin class of inhibitors and also termed nodularin-V due to the valine in its variable position, Figure 1(b)), was identified from the marine sponge *Theonella swinhoei*.[12]

Previously the solution structures of microcystin-LR (MCLR, L=leucine and R=arginine in two variable positions) and of MOT using $^{1}$H nuclear

Abbreviations used: PP-1c, protein phosphatase-1; Masp, D-erythro-β-methyl aspartic acid; MOT, motuporin; Adda, 3-amino-9-methoxy-2,6,8-trimethyl-10-phenyl-deca-4,6-dienoic acid; OA, okadaic acid; Nmda, *N*-methyldehydroalanine; MC-LR, microcystin-LR.

E-mail address of the corresponding author: charles.holmes@ualberta.ca

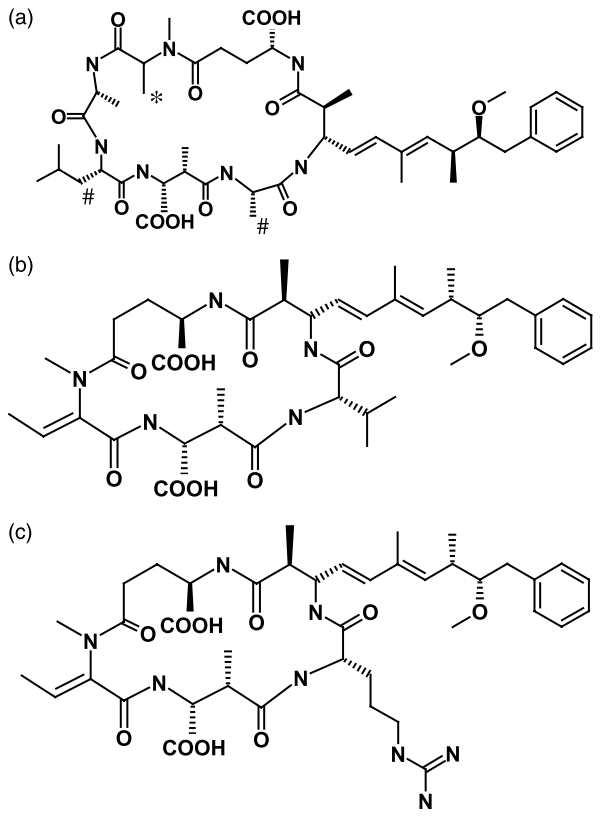


**Figure 1.** Chemical structure of the cyanobacterial toxins. (a) Structure of dihydromicrocystin-LA (MCLA-2H). #The two sites of modification for the microcystins, in MCLA-2H these sites are Leu and Ala and in MCLR these sites are Leu and Arg. *The site of hydrogenation that removes the *N*-methyldehydroalanine residue and creates an *N*-methylalanine residue with no Michael addition properties. The 3-amino-9-methoxy-2,6,8-trimethyl-10-phenyl-deca-4,6-dienoic acid (Adda) residue includes all of the hydrophobic tail region of the inhibitor. (b) Structure of motuporin (nodularin-V). The Adda residue includes all of the hydrophobic tail region of the inhibitor. (c) Structure of nodularin-R.

magnetic resonance spectroscopy were determined.[13] Subsequently, the solution structure of the related nodularin-R (variable amino acid is arginine, Figure 1(c)) was also elucidated.[14] The peptide ring of MCLR has a saddle-shaped motif with carboxyl residues as stirrups at the sides. Both the 3-amino-9-methoxy-2,6,8-trimethyl-10-phenyl-deca-4,6-dienoic acid (Adda) and arginine side-chains are highly flexible, whereas the leucine side-chain of the toxin is well defined. The cyclic peptide ring of MOT forms a smaller, well-defined saddle shape having less pucker than MCLR.

Determination of the crystal structure of MCLR bound to PP-1c (α isoform) showed that the toxin binds to PP-1c through interactions with three regions of the phosphatase[15] including the active site with the two catalytic metals, the hydrophobic groove and the $\beta_{12}$-$\beta_{13}$ loop region. Microcystin-LR coordinates with the two catalytic metal atoms of the phosphatase indirectly by binding two water molecules through the α-carboxyl group of its γ-linked D-glutamic acid moiety and the adjacent carbonyl oxygen. This accounts for the observation that the glutamic acid α-carboxyl group is absolutely necessary for toxicity of the cyclic peptide.[6] In addition, the carboxyl group of the Masp residue of MCLR interacts with Arg96 and Tyr134 of PP-1c. Thus, MCLR completely blocks access to the active centre of the enzyme.[16] The long hydrophobic tail, composed of the Adda residue of MCLR, is placed in the hydrophobic groove region of PP-1c, adjacent to the active site.

Interactions of cyclic peptide toxins also occur at the toxin-sensitive $\beta_{12}$-$\beta_{13}$ loop (residues 268–281) of PP-1c. A covalent linkage between the Nmda side-chain of the toxin and the sulphur of C273 of PP-1c was observed in the crystal structure, verifying earlier biochemical analyses.[17–21] This covalent reaction most likely proceeds *via* a Michael addition type-reaction to the double bond of Nmda. Comparison of the crystal structures of PP-1c with and without MCLR bound[22,23] suggested that the $\beta_{12}$-$\beta_{13}$ loop of PP-1c shifts to avoid steric conflict between Tyr272 and the Nmda residue of the toxin. This observation first suggested that flexibility of the $\beta_{12}$-$\beta_{13}$ loop might be important for toxin binding and inhibition of the enzyme. However, the covalent linkage that occurs is secondary to the inhibitor activity of the toxin and likely occurs as a delayed reaction in solution. The biological relevance of this reaction is unknown.

Whilst sharing similar biological properties, important functional differences exist between the microcystins and nodularins with respect to their interaction with PP-1c/PP-2Ac. Although both toxins initially bind non-covalently and inhibit these enzymes, the nodularins, including MOT, do not bind covalently to PP-1c/PP-2Ac even as a delayed reaction.[17,18] This is despite possessing an *N*-methyldehydrobutyrine residue that could undergo a Michael addition reaction with C273 similar to the reaction of the Nmda residue in MCLR.

Recently, the crystal structures of PP-1cγ bound to two other natural toxins (okadaic acid (OA) and calyculin) have been determined.[24,25] The overall structure of PP-1c in all of these complexes is similar to PP-1cα in the PP-1c:MCLR complex, except for prominent differences in the orientation of the $\beta_{12}$-$\beta_{13}$ loop region. These findings suggested that the different orientation of the $\beta_{12}$-$\beta_{13}$ loop in the PP-1c:MCLR complex[15] may have been solely due to the unusual covalent binding between C273 of PP-1c and MCLR. In order to verify this hypothesis we have determined the structure of PP-1cγ bound to MOT, which, besides being a novel inhibitor of PP-1c, possesses a dehydrobutyrine residue that could potentially undergo a Michael addition reaction with C273, similar to the microcystins. We have also determined the structure of a microcystin congener (dihydromicrocystin-LA(MCLA-2H); Figure 1(a)) in which the Nmda residue has been hydrogenated, thereby removing the ability

of the microcystin to form a covalent bond with C273 of PP-1c.

## Results

### Structure of motuporin (nodularin-V) bound to PP-1c

The toxins of PP-1c contain three common features: a carboxyl group, a hydrophobic tail and a large macrocyclic domain (the macrocycle is created *via* an intramolecular hydrogen bond in OA). Motuporin binds to PP-1c in a manner similar to other toxins in that its macrocyclic ring occupies most of the active site region and its hydrophobic tail occupies the hydrophobic groove region of PP-1c that is adjacent to the active site (Figure 2). The α-carboxyl moiety from the γ-linked D-glutamic acid of MOT lies in proximity to similar organic acids from MCLR and OA and to the phosphate from calyculin A. These negatively charged groups serve to bind indirectly to the active site metals of the enzyme *via* bridging water molecules.

The hydrophobic tail of MOT, composed of the long Adda side-chain, primarily interacts with residues W206, V223 and I130 of PP-1c (Figure 2). There are a significant number of hydrogen bonding contacts between MOT and PP-1c, including strong interactions with Arg96 (three potential bonds, all involving guanidinium nitrogen atoms), Y134, R221 and Y272 (Figure 2(a)). These interactions include the conserved carboxylate motif present in the γ-linked glutamic acid and the carboxylate of the Masp residue. Motuporin interacts with the active site metals indirectly through a hydrogen bond to a bridging water. In comparison with the previous MCLR structure where the dehydroalanine residue reacted with C273, the dehydrobutyrine residue of MOT is 4.7 Å from the cysteine and forms no covalent adduct.

The structure of MOT bound to PP-1c is quite different from the minimized average solution structure determined by NMR (RMSD of 1.7 Å over 55 atoms) (Figure 3(a)).[13] This is in contrast to the similarity of PP-1c-bound and free structures observed for OA (RMSD of 0.7 Å over 70 atoms of the toxin in a comparison of the bound and unbound crystal structures)[25] but similar to MCLR (RMSD of 1.8 Å over 57 atoms in a comparison of PP-1-bound crystal and the unbound NMR minimal-averaged structure).[15]

### Structure of dihydromicrocystin-LA bound to PP-1c

Dihydromicrocystin-LA binds to PP-1c in a similar manner to its congener MCLR (Figures 4 and 5) with the notable exception being the lack of a covalent interaction with C273 in the $\beta_{12}$-$\beta_{13}$ loop of the phosphatase. Significantly, this loop adopts a very different conformation in the absence of a covalent bond with the toxin. The distance between C273 and the hydrogenated Nmda residue is 8.2 Å. In addition, there are hydrogen bonding contacts between MCLA-2H and PP-1c including interactions with Y134, R221 and Y272 (Figure 4(a)). Of note is the lack of a hydrogen bond between Arg96 and the γ-linked glutamic acid, which is present in the PP-1c:MOT complex (Figure 2).

### Comparison of PP-1c structures bound to motuporin, dihydromicrocystin-LA and microcystin-LR

Comparison of PP-1c structures with different toxins bound reveals overall similarity in the enzyme structures. The structure of PP-1c bound to MCLA-2H has a $C^{\alpha}$ RMSD value of 0.3 Å (over 293 atoms, including the $\beta_{12}$-$\beta_{13}$ loop) when compared with the PP-1c:OA complex and 0.5 Å (over the same 293 atoms) when compared with the PP-1c:MCLR complex. The equivalent values for the PP-1c:MOT complex are 0.3 Å and 0.5 Å for the OA and MCLR complexes, respectively. However, comparison of PP-1c structures bound to MOT, MCLA-2H and MCLR illustrate a significant change in the conformation of the toxin-sensitive $\beta_{12}$-$\beta_{13}$ loop due to covalent modification of C273 in PP-1c (Figure 5). The $C^{\alpha}$ RMSD value over residues 270–276 of the loop region is 2.0 Å for comparison of the MCLR complex to both the MCLA-2H and MOT complexes. This contrasts with a $C^{\alpha}$ RMSD value of 0.1 Å when comparing the equivalent regions of the MCLA-2H and MOT complexes. The conformation of this loop is identical in the structures of PP-1c bound to MOT and MCLA-2H; however, it is substantially shifted in the MCLR complex.

## Discussion

The PP-1c:MOT structure presented here is the fourth novel PP-1c-toxin structure to be elucidated.[15,24,25] Each determined structure is sufficiently unique to contribute to the hypothesis that toxin/substrate binding to PP-1c can occur by a multitude of modes. The hydrophobic tail of MOT does not interact with PP-1c as intimately as the corresponding hydrophobic portion of OA, as illustrated by the higher thermal coefficients and poorer electron density of the region. The average thermal factor for the atoms of the hydrophobic tail of the Adda residue of MOT is 5.8 $Å^2$ greater than the average thermal factor for the entire inhibitor. The equivalent hydrophobic tail atoms of OA have an average thermal factor 1.3 $Å^2$ above the average thermal factor for the entire inhibitor. The hydrophobic tail of OA has five potential van der Waals interactions with the hydrophobic groove that are within 4 Å, whereas MOT only has two potential interactions.

The macrocylic ring portion of OA that occupies the active site region of PP-1c has very few hydrogen bonding interactions with the enzyme and therefore hydrophobic binding may provide

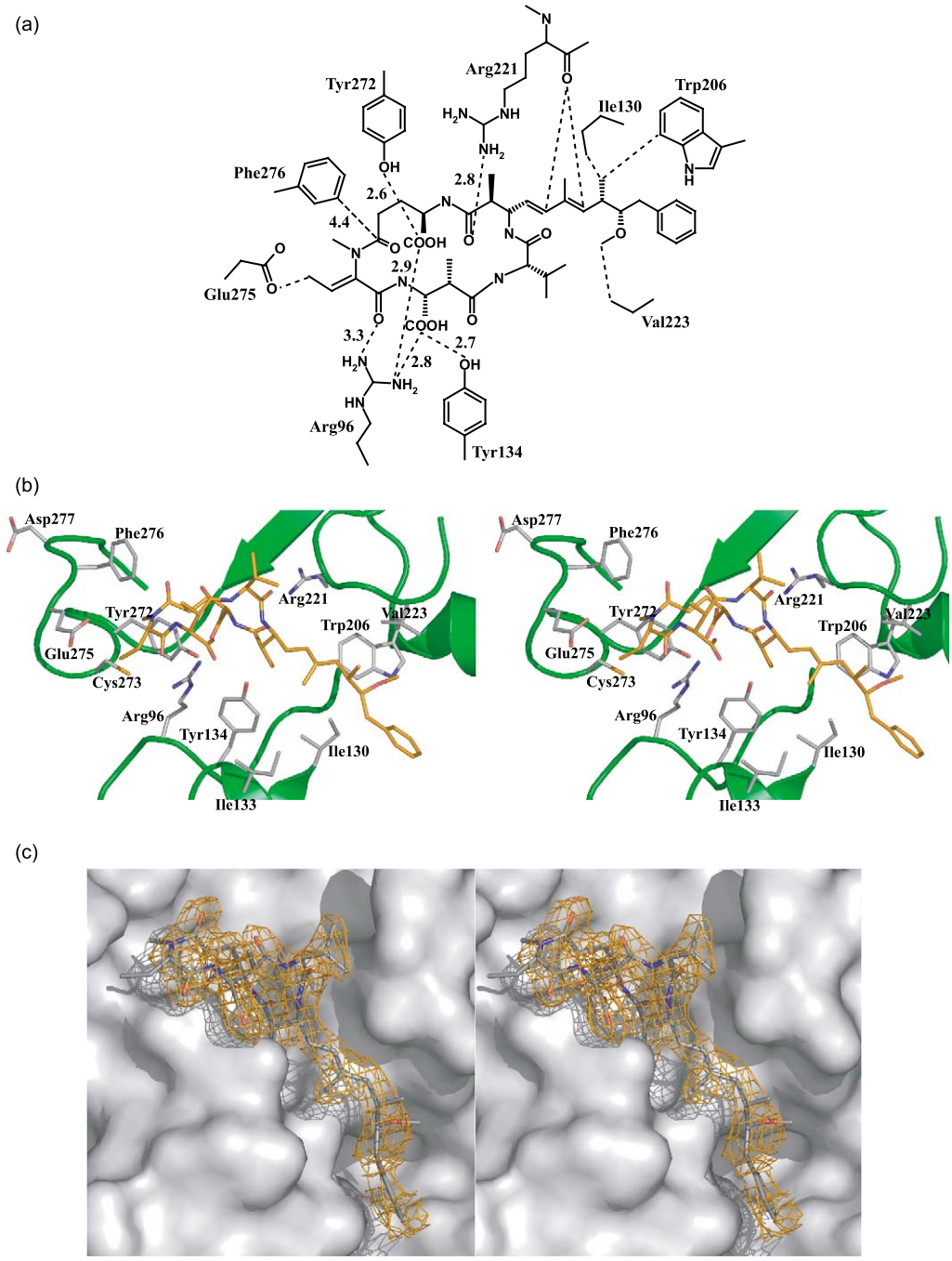


**Figure 2.** Crystal structure of motuporin bound to protein phosphatase-1c. (a) Structural formula representation of MOT showing active site contacts with PP-1c within 4 Å. All potential hydrogen bonds have their distances shown. (b) Stereo representation of the active site contacts in the crystal structure of MOT bound to PP-1c. The enzyme is shown as a green backbone ribbon trace with grey carbon atoms on the side-chains of pertinent residues. Motuporin is displayed as sticks with orange carbon atoms. (c) Stereo representation of the electron density seen for MOT superimposed on the surface of PP-1c (colored grey). All density shown is a $\sigma_A$-weighted $2F_o - F_c$ map contoured at 1σ.

the larger proportion of the binding energy (two potential hydrogen bonds exist between the inhibitor and the enzyme, both of which are relatively distant, being close to or greater than 3 Å in length, with putative donor-hydrogen acceptor hydrogen bond angles of 134° and 147° (defined as the putative donor–hydrogen-acceptor angle). Motuporin has considerably more hydrogen bonds between the enzyme and the macrocylic ring, specifically the two acidic moieties of the ring, and therefore could rely less on hydrophobic binding energy (five potential hydrogen bonds exist between the inhibitor and the enzyme, three of which are relatively strong, being $<2.9$ Å in length, hydrogen bond angles between 102° and 153°). The comparison of enzyme-bound and free inhibitor structures also shows evidence of this. It was noted previously that the bound and

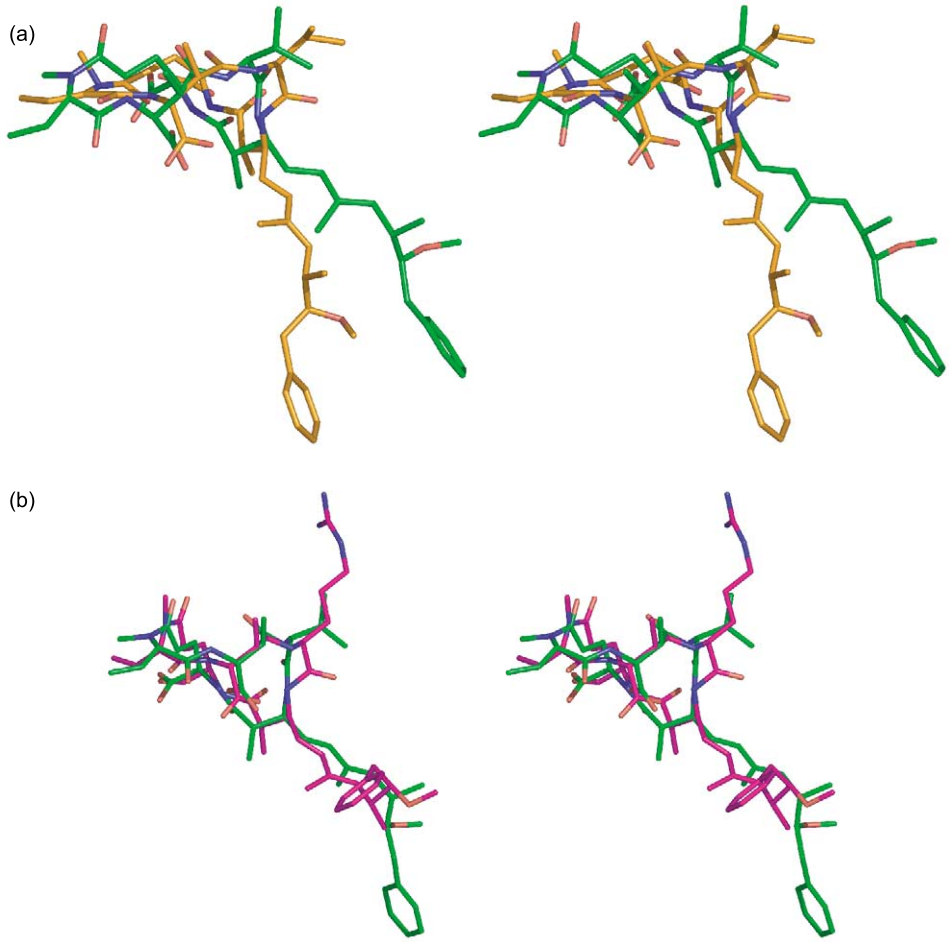


**Figure 3.** Superimposition of the determined nodularin structures. (a) Overlay of the MOT structure bound to PP-1c, as determined by X-ray crystallography (green) and solution MOT structure as determined by NMR (orange).[13] Orientation of the inhibitors is the same as in Figure 2. (b) Overlay of the MOT (nodularin-V) structure bound to PP-1c, as determined by X-ray crystallography (green) and a solution structure of nodularin-R.[14] Orientation of the inhibitors is the same as in Figure 2.

free structures of OA are virtually identical and therefore the entropic cost of binding is minimized.[25] A similar observation was made for the enzyme-bound and NMR solution structure of MCLR.[13] When comparing the solution NMR structure of MOT with the enzyme-bound structure, differences in the ring region and flexibility in the hydrophobic tail region are noted (Figure 3(a)).[13] A second comparison to the NMR solution structure of a related nodularin (nodularin-R) shows similar flexibility in the tail region (Figure 3(b)).[14] As evidence that OA relies more on hydrophobic binding and entropy, the buried protein surface area that OA occupies is 738 $Å^2$, where as MOT only occupies 500 $Å^2$. Taken together this evidence shows that MOT most likely relies less on hydrophobic binding energy and minimizing the entropic cost of binding than does OA and MCLR. Instead, MOT has numerous hydrogen bonding interactions with the enzyme that compensate for the lack of the former interactions. The increased hydrogen bonding interaction between MOT and PP-1c may explain the increased potency of this toxin towards PP-1c when compared with OA ($IC_{50}$ = 0.06 nM *versus* 20 nM, respectively).

In the complexes of PP-1c with MCLA-2H and MOT, Y272 functions as a hydrogen bonding partner with an acid moiety of the inhibitors. In this capacity, the function of the tyrosine is equivalent for both the MCLA-2H and MOT. Previous kinetic data showed that mutation of Y272 affected the two inhibitors to significantly different degrees.[26] Abolition of the hydrogen bonding capacity but maintenance of the large size of tyrosine by mutation to phenylalanine or tryptophan had virtually no effect on the affinity of PP-1c for either inhibitor, suggesting that the hydrogen bond from Y272 to the inhibitor carboxylate may not be overly important (the same carboxyl group of the inhibitor also functions to bind the catalytic metals of the phosphatase indirectly *via* bridging water molecules). However, mutation of this tyrosine to other amino acids of varying chemical properties had quite different results. Replacement of the tyrosine with alanine, serine/threonine, cysteine, glutamate or lysine typically increased the $IC_{50}$ value of MCLR by 10 to 50-fold whereas the same substitutions for nodularin-R increased the $IC_{50}$ values by 150–250-fold. This

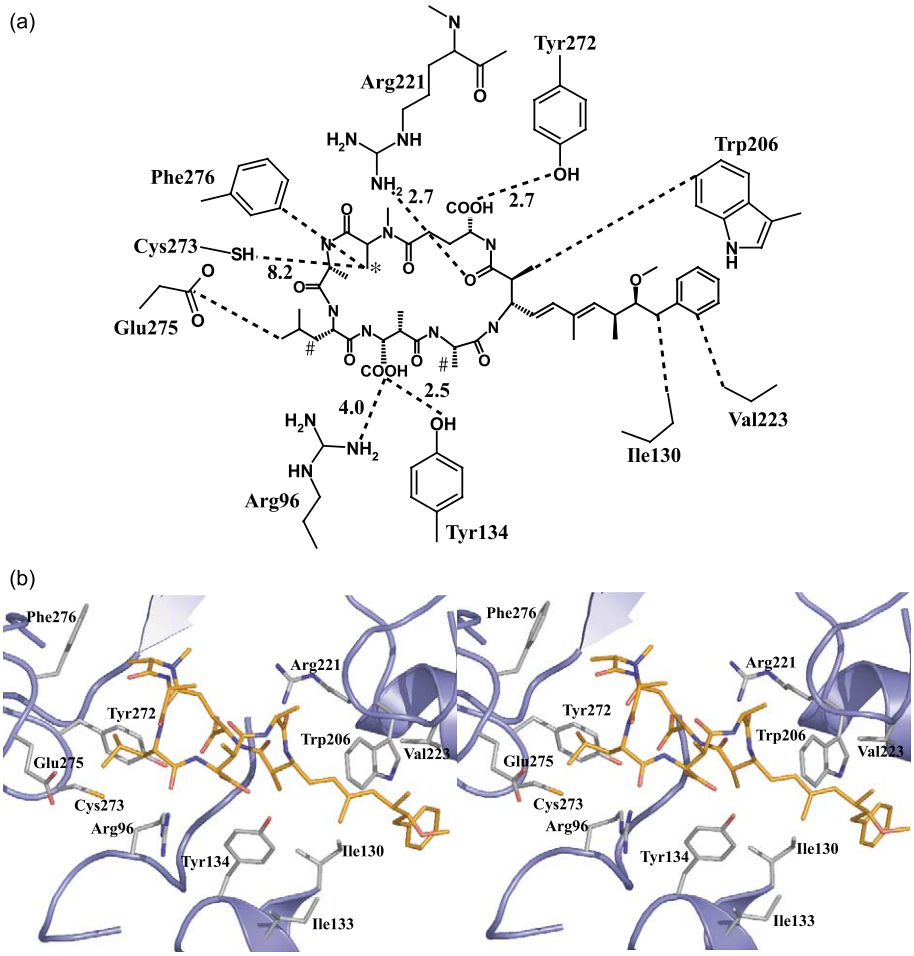


**Figure 4.** Crystal structure of MCLA-2H bound to protein phosphatase-1c. (a) Linear representation of MCLA-2H showing active site contacts within 4 Å. All potential hydrogen bonds have their distances shown. Toxin is labelled as for Figure 1. (b) Stereo representation of the active site contacts in the crystal structure of MCLA-2H bound to PP-1c. The enzyme is shown as a blue backbone ribbon trace with grey carbon atoms for the side-chains of pertinent residues. Motuporin is displayed as sticks with orange carbon atoms.

tyrosine occupies a noteworthy position in the enzyme active site, near the catalytic metals and at the base of the hinge of the $\beta_{12}$-$\beta_{13}$ loop region. In the apoenzyme form, Y272 most likely does not have a hydrogen-bonding partner, other than metal-bound water molecules. It most likely is more important in creating the hydrophobic surface of the $\beta_{12}$-$\beta_{13}$ loop region and maintaining its position. Removal of the tyrosine might allow for greater movement of the loop. This is consequential for the microcystins, since they possess a significant number of potential contacts in the region of the $\beta_{12}$-$\beta_{13}$ loop (Figure 4). Motuporin does not have this capacity, since its macrocyclic ring does not lie in proximity to the rest of the $\beta_{12}$-$\beta_{13}$ loop. This may explain why mutations of Y272 affect MOT to a larger degree than do the microcystins.

Significant differences exist in the mechanism of PP-1c binding between the motuporin/nodularin class and the microcystin class of cyanobacterial toxins in that the nodularin cyanotoxins do not bind covalently to their enzyme target. This occurs despite the presence of residues in both classes that could participate in Michael addition reactions (*N*-methyldehydroalanine in the microcystins and *N*-methyldehydrobutyrine in MOT). Determination of the crystal structure of MOT bound to PP-1c provides a molecular explanation for the lack of covalent binding to the phosphatase. The reactive residue in PP-1c, C273, is not orientated sufficiently close to *N*-methyldehydrobutyrine to enable covalent binding to occur. The lack of proximity of the sulphur nucleophile of C273 may disrupt the Burgi–Dunitz angle of approach necessary to obtain a covalent Michael addition with this residue in MOT.[27] While the lack of covalent modification affects the final complex that exists between MOT and the cognate enzyme, it is unlikely to affect the inhibitory potential of MOT, since the covalent reaction observed with MCLR was shown to differ temporally from initial inhibition of PP-1c.[17]

Comparison of PP-1c structures bound to MOT, MCLA-2H and MCLR illustrates a significant change in the conformation of the toxin-sensitive $\beta_{12}$-$\beta_{13}$ loop due to the covalent modification of C273 in PP-1c. The conformation of this loop is

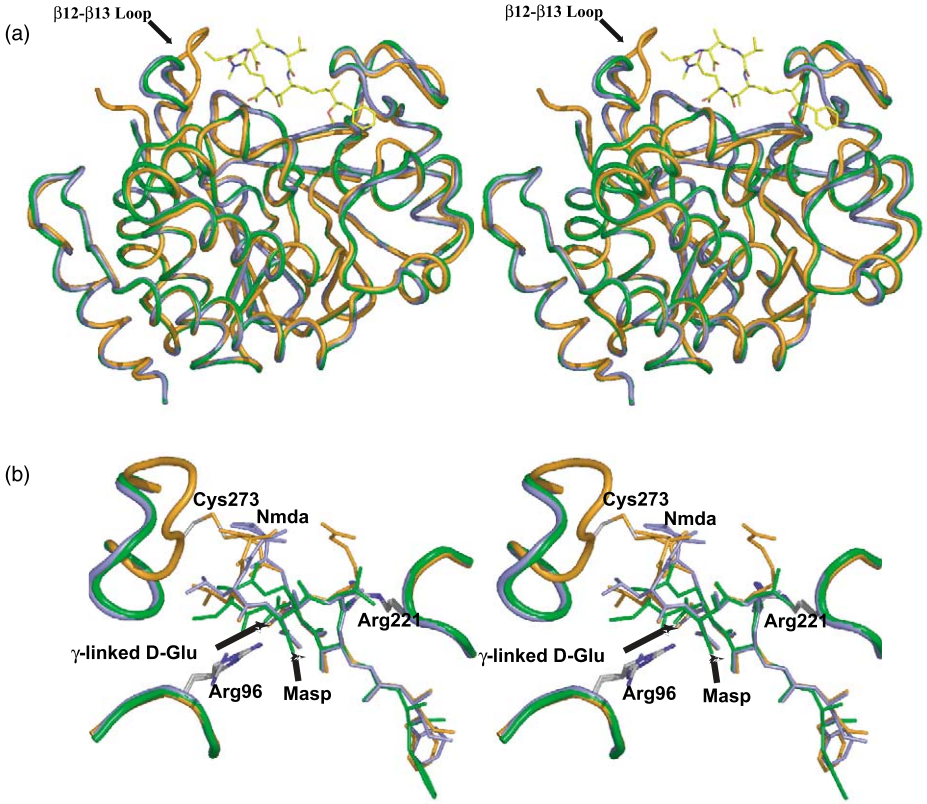


**Figure 5.** Comparison of PP-1c structures bound to toxins. (a) Stereo representation of the overlay of PP-1c bound to MCLA-2H (blue), MOT (green) and MCLR (orange).[15] Motuporin is shown as sticks and the $\beta_{12}$-$\beta_{13}$ loop is labeled. (b) Stereo representation of the active site regions of the PP-1c-bound toxin structures. The β-methylaspartic acid (Masp), γ-linked D-glutamic acid and *N*-methyldehydroalanine (Nmda) residues are labeled. In MCLA-2H, the *N*-methylalanine residue and in MOT, the *N*-methyldehydrobutyrine residues are both in the equivalent position to Nmda. The disulphide bond between the Nmda residue of MCLR and C273 is shown. Colouring is the same as in (a).

identical in the presence of either MOT or non-covalently bound MCLA-2H (Figure 5), but changes substantially with the formation of the Michael addition complex between Nmda of MCLR and C273. Determination of the PP-1c structure bound to MCLA-2H shows conclusively that the change in the $\beta_{12}$-$\beta_{13}$ loop conformation in the PP-1c:MCLR complex is due to the formation of a covalent bond between the phosphatase and bound toxin. Presumably, it is possible for the Michael addition reaction to occur without significant loop movement and, therefore, the loop rearrangement most likely occurs after the Michael addition reaction has taken place.

Previously, site-directed mutagenesis has shown that the initial non-covalent interactions between C273 and the microcystins contribute to the initial and rapid inhibition (in min) of PP-1c prior to a much slower covalent modification step. Runnegar *et al.*[19] and MacKintosh *et al.*[18] independently showed that PP-1c binds covalently to MCLR, confirming modification of the *N*-methyldehydroalanine moiety of microcystin with PP-1c at C273.[28] Covalent binding of microcystins to PP-1c is not observed when the phosphatase is denatured,[18] indicating that the interaction depends on an intact active site.[28]

MacKintosh *et al.*[18] determined that mutation of C273 to Ser or Leu increased the $IC_{50}$ for toxin inhibition of PP-1c by ten and 20-fold, respectively, as well as abolishing covalent binding. Mutagenesis of residues 273–277 of the β12-β13 loop of PP-1c to the corresponding residues (L273, D274, V275, Y276 and N277) from the related phosphatase calcineurin by Maynes *et al.* resulted in a chimeric mutant that showed a similarly increased 20-fold resistance to microcystin inhibition.[29] Determination of the crystal structure of this PP-1c-calcineurin hybrid and systematic mutation of each of the five residues in the β12-β13 loop, confirmed that a single amino acid change (C273L) and not a change in the overall β12-β13 loop conformation, was the most influential factor in the increased toxin resistance exhibited by mutation of C273.[29]

Several studies have suggested that the *N*-methyldehydroalanine residue in microcystins does not play a role in the initial enzyme-inhibitor interactions. Microcystins immobilized to Sepharose beads *via* an aminoethanethiol adduct retain PP-1c inhibitory activity.[30] Conversion of MCLR to a microcystin-glutathione conjugate *via* Michael addition to the *N*-methyldehydroalanine residue diminished its *in vivo* toxicity in animal models, but did not abolish it ($LD_{50}$ = 630 μg per kg *versus* 38 μg

per kg for microcystin-LR, respectively).[31] Finally, Craig *et al*. confirmed a two step mechanism for irreversible protein phosphatase inhibition by microcystins.[17,28] Kinetically, covalent modification of C273 (and the analogous residue C266 in the related protein phosphatase PP-2A) occurs slowly over several hours.[17,28] This contrasts with the initial rapid non-covalent binding and inhibition of the enzyme by multiple toxin interactions described here. Taken together, our crystal structures show that these interactions must first occur with the β12-β13 loop in the same position as the previously determined PP-1c-OA and calyculin complexes.[24,25] This is entirely consistent with our previous conclusion that stoichiometric formation of a covalent complex adventitiously follows after prolonged incubation of toxin and phosphatase.[16,17]

Evidence has been obtained for the persistent presence of covalent complexes between PP-1c and MCLR *in vivo* in microcystin-poisoned salmon afflicted by netpen liver disease,[32] in salt water mussels[33] and in microcystin-poisoned trout.[34] Therefore, although not required for protein phosphatase inhibition, covalent modification may play a role in the bioavailability of the toxin and may influence temporally distinct signalling pathways involving Ser/Thr protein phosphatases.[32,34]

The data presented here suggest that non-covalently bound complexes of phosphatase and toxin (MOT) also have the potential to be toxic, since the nodularins possess similar toxicity to the microcystins.[1,6,10] Additional support for this hypothesis has recently been obtained by Hastie *et al*.,[35] who have reported that the dehydrobutyrine (Dhb)-containing microcystin variant [3-Asp, 5-ADMAAdda, 7-Dhb]microcystin-HtyR from *Nostoc* sp. does not interact covalently with PP-2A, yet is as potent a PP-1c inhibitor as MCLR and almost as toxic ($LD_{50}$ = 100 μg per kg).

## Experimental Procedures

### Purification of natural product toxins

Microcystin-LA was purified from natural blooms of *Microcystis aeruginosa* using procedures described.[17] Motuporin was purified and characterised as described by Desilva *et al*.[12] Site-specific reduction of MCLA by $NaBH_4$ was carried out as described;[17] the final product was fully characterized by high resolution mass spectrometry (FABMS) and $^1$H-NMR analysis(data not shown).

### Crystallization

The catalytic subunit of human protein phosphatase-1γ was purified as described.[17,25] Crystals were obtained by co-crystallization using the hanging-drop vapor-diffusion method at room temperature. For both MOT and MCLA-2H, the enzyme and inhibitor were mixed in a 1:3 molar ratio with the final concentration of protein being 12 mg/ml. The PP-1c inhibitor complexes were then mixed with an

**Table 1.** Data collection and refinement statistics

| | PP-1c–MOT complex | PP-1c–MCLA–2H complex |
|---|---|---|
| *Data collection* | | |
| Unit cell | $a=b=101.0$ Å, $c=63.49$ Å, $\alpha=\beta=\gamma=90°$ | $a=b=100.0$ Å, $c=62.9$ Å, $\alpha=\beta=\gamma=90°$ |
| Space group | $P4_22_12$ | $P4_22_12$ |
| Wavelength (Å) | 1.00 | 1.00 |
| Resolution (Å)[a] | 40–2.1 (2.20–2.10) | 40–2.3 (2.42–2.30) |
| Total number of reflections | 186,190 | 113,187 |
| Number of unique reflections | 19,726 | 14,724 |
| Completeness (%)[a] | 99.9 (99.9) | 99.9 (99.9) |
| Redundancy[a] | 3.7 (3.8) | 7.7 (7.6) |
| $\langle I/\sigma(I)\rangle$[a] | 13.5 (4.6) | 20.4 (6.7) |
| $R_{sym}$ (%)[a,b] | 6.5 (29.3) | 7.2 (28.7) |
| Mosaicity (deg.) | 0.37 | 0.52 |
| *Refinement* | | |
| Resolution (Å) | 40–2.1 | 40–2.3 |
| Protein atoms | 2350 | 2338 |
| Waters | 73 | 35 |
| r.m.s. deviations | | |
| Bond length (Å) | 0.02 | 0.013 |
| Bond angles (deg.) | 1.84 | 1.57 |
| Average *B*-factors | | |
| Protein atoms (Å$^2$) | 26.3 | 32.7 |
| Inhibitor atoms (Å$^2$) | 32.3 | 43.7 |
| Solvent (Å$^2$) | 29 | 30.1 |
| $R_{cryst}$ (%)[c] | 0.22 | 0.21 |
| $R_{free}$ (%)[d] | 0.26 | 0.25 |

[a] Data in parentheses correspond to highest resolution shell.
[b] $R_{sym} = \Sigma|I-\langle I\rangle|/\Sigma\langle I\rangle$, where $I$ is the observed intensity and $\langle I\rangle$ is the average intensity obtained from multiple observations of symmetry-related reflections.
[c] $R_{free}$ was calculated as for $R_{cryst}$ with the 5% of the data omitted from structural refinement.
[d] $R_{cryst} = \Sigma||F_o|-|F_c||/\Sigma|F_o|$, where $|F_o|$ and $|F_c|$ are the observed and calculated structure factor amplitudes, respectively.

equivalent volume of mother liquor, that consisted of 2.3 M lithium sulfate, 100 mM Tris–HCl (pH 8.0), 2% (w/v) polyethylene glycol 400 and 10 mM β-mercaptoethanol. Both complexes crystallized in the space group $P4_22_12$ with one complex per asymmetric unit. The crystal data for both complexes are given in Table 1.

### Data collection, structure determination and refinement

The X-ray diffraction data for both complexes were collected at Beamline 8.3.1 at the Advanced Light Source in Berkeley, California on an ADSC Q210 detector. All data were collected at 1 Å wavelength. The data were processed using the programs MOSFLM[36] and SCALA.[37] Both structures were solved by molecular replacement with the program AMoRe[38] using the structure of PP-1c as determined in the complex bound to OA[25] as the starting model. The electron densities for the protein and bound inhibitors were clear in both instances (Figure 2(c)). The protein-inhibitor model was fitted manually using the program XtalView.[39] The starting model for MOT came from the NMR structure of the inhibitor[13] and the starting model for MCLA-2H came from the previous crystal structure of MCLR bound to PP-1c.[15] The structural models were subjected to iterative rounds of macromolecular refinement using the program REFMAC[40] with a maximum likelihood target. The crystallographic data are listed in Table 1. The final structures consisted of PP-1c residues 6 through 298 and complete inhibitor models for both complexes. The models were checked for validity using the programs WHATCHECK[41] and PROCHECK.[42] The final PP1:MOT structure had 97.3% of residues in allowed Ramachandran plot regions with a *G*-factor of −0.2. The final PP1:MCLA-2H structure had 97.7% of residues in allowed Ramachandran plot regions with a *G*-factor of −0.1.

### Protein Data Bank accession codes

The atomic coordinates and structure factors have been deposited in the RCSB Protein Data Bank with accession codes 2BCD (PP-1:MOT) and 2BDX (PP-1:MCLA-2H).

## Acknowledgements

J.T.M. is a Pfizer MD/PhD Student and M.N.G.J. holds a Canada Research Chair in Protein Structure and Function. Supported by Canadian Institutes of Health Research operating grants to C.F.B.H. and M.N.G.J. C.F.B.H. is an Alberta Heritage Foundation for Medical Research Scientist.

## References

1. Carmichael, W. W. (1994). Toxins of cyanobacteria. *Sci. Am.* **270**, 78–86.
2. Yoshizawa, S., Matsushima, R., Watanabe, M. F., Harada, K., Ichihara, A., Carmichael, W. W. & Fujiki, H. (1990). Inhibition of protein phosphatases by microcystis and nodularin associated with hepatotoxicity. *J. Cancer Res. Clin. Oncol.* **116**, 609–614.
3. Honkanen, R. E., Zwiller, J., Moore, R. E., Daily, S. L., Khatra, B. S., Dukelow, M. & Boynton, A. L. (1990). Characterization of microcystin-LR, a potent inhibitor of type-1 and type-2a protein phosphatases. *J. Biol. Chem.* **265**, 19401–19404.
4. MacKintosh, C., Beattie, K. A., Klumpp, S., Cohen, P. & Codd, G. A. (1990). Cyanobacterial microcystin-LR is a potent and specific inhibitor of protein phosphatases 1 and 2A from both mammals and higher plants. *FEBS Letters*, **264**, 187–192.
5. Nishiwaki-Matsushima, R., Nishiwaki, S., Ohta, T., Yoshizawa, S., Suganuma, M., Harada, K. *et al*. (1991). Structure–function-relationships of microcystins, liver-tumor promoters, in interaction with protein phosphatase. *Jpn. J. Cancer Res.* **82**, 993–996.
6. Holmes, C. F. B. & Boland, M. P. (1993). Inhibitors of protein phosphatase-1 and phosphatase-2a. Two of the major serine threonine protein phosphatases involved in cellular regulation. *Curr. Opin. Struct. Biol.* **3**, 934–943.
7. Eriksson, J. E., Toivola, D., Meriluoto, J. A. O., Karaki, H., Han, Y. G. & Hartshorne, D. (1990). Hepatocyte deformation induced by cyanobacterial toxins reflects inhibition of protein phosphatases. *Biochem. Biophys. Res. Commun.* **173**, 1347–1353.
8. Ohta, T., Nishiwaki, R., Yatsunami, J., Komori, A., Suganuma, M. & Fujiki, H. (1992). Hyperphosphorylation of cytokeratins 8 and 18 by microcystin-LR, a new liver-tumor promoter, in primary cultured rat hepatocytes. *Carcinogenesis*, **13**, 2443–2447.
9. Craig, M., McCready, T. L., Luu, H. A., Smillie, M. A., Dubord, P. & Holmes, C. F. B. (1993). Identification and characterization of hydrophobic microcystins in Canadian fresh-water cyanobacteria. *Toxicon*, **31**, 1541–1549.
10. Rinehart, K. L., Harada, K., Namikoshi, M., Chen, C., Harvis, C. A. *et al*. (1988). Nodularin, microcystin, and the configuration of adda. *J. Am. Chem. Soc.* **110**, 8557–8558.
11. Ohta, T., Nishiwaki, R., Suganuma, M., Yatsunami, J., Komori, A., Okabe, S. *et al*. (1993). Significance of the cyanobacterial cyclic peptide toxins, the microcystins and nodularin, in liver-cancer. *Mutat. Res.* **292**, 286–287.
12. Desilva, E. D., Williams, D. E., Andersen, R. J., Klix, H., Holmes, C. F. B. & Allen, T. M. (1992). Motuporin, a potent protein phosphatase inhibitor isolated from the Papua-New-Guinea sponge *Theonella swinhoei* Gray. *Tetrahedron Letters*, **33**, 1561–1564.
13. Bagu, J. R., Sonnichsen, F. D., Williams, D., Andersen, R. J., Sykes, B. D. & Holmes, C. F. B. (1995). Comparison of the solution structures of microcystin-LR and motuporin. *Nature Struct. Biol.* **2**, 114–116.
14. Annila, A., Lehtimaki, J., Mattila, K., Eriksson, J. E., Sivonen, K., Rantala, T. T. & Drakenberg, T. (1996). Solution structure of nodularin. An inhibitor of serine/threonine-specific protein phosphatases. *J. Biol. Chem.* **271**, 16695–16702.

15. Goldberg, J., Huang, H. B., Kwon, Y. G., Greengard, P., Nairn, A. C. & Kuriyan, J. (1995). Three-dimensional structure of the catalytic subunit of protein serine/threonine phosphatase-1. *Nature*, **376**, 745–753.
16. Holmes, C. F. B., Maynes, J. T., Perreault, K. R., Dawson, J. F. & James, M. N. G. (2002). Molecular enzymology underlying regulation of protein phosphatase-1 by natural toxins. *Curr. Med. Chem.* **9**, 1981–1989.
17. Craig, M., Luu, H. A., McCready, T. L., Williams, D., Andersen, R. J. & Holmes, C. F. B. (1996). Molecular mechanisms underlying he interaction of motuporin and microcystins with type-1 and type-2A protein phosphatases. *Biochem. Cell Biol.* **74**, 569–578.
18. MacKintosh, R. W., Dalby, K. N., Campbell, D. G., Cohen, P. T., Cohen, P. & MacKintosh, C. (1995). The cyanobacterial toxin microcystin binds covalently to cysteine-273 on protein phosphatase 1. *FEBS Letters*, **371**, 236–240.
19. Runnegar, M., Berndt, N., Kong, S. M., Lee, E. Y. C. & Zhang, L. F. (1995). *In vivo* and *in vitro* binding of microcystin to protein phosphatase-1 and phosphatase-2a. *Biochem. Biophys. Res. Commun.* **216**, 162–169.
20. Dawson, J. F. & Holmes, C. F. B. (1999). Molecular mechanisms underlying inhibition of protein phosphatases by marine toxins. *Front. Biosci.* **4**, D646–D658.
21. McCluskey, A., Sim, A. T. R. & Sakoff, J. A. (2002). Serine-threonine protein phosphatase inhibitors: development of potential therapeutic strategies. *J. Med. Chem.* **45**, 1151–1175.
22. Egloff, M. P., Cohen, P. T., Reinemer, P. & Barford, D. (1995). Crystal structure of the catalytic subunit of human protein phosphatase 1 and its complex with tungstate. *J. Mol. Biol.* **254**, 942–959.
23. Barford, D. (1996). Molecular mechanisms of the protein serine threonine phosphatases. *Trends Biochem. Sci.* **21**, 407–412.
24. Kita, A., Matsunaga, S., Takai, A., Kataiwa, H., Wakimoto, T., Fusetani, N. *et al*. (2002). Crystal structure of the complex between calyculin A and the catalytic subunit of protein phosphatase 1. *Structure*, **10**, 715–724.
25. Maynes, J. T., Bateman, K. S., Cherney, M. M., Das, A. K., Luu, H. A., Holmes, C. F. B. & James, M. N. G. (2001). Crystal structure of the tumor-promoter okadaic acid bound to protein phosphatase-1. *J. Biol. Chem.* **276**, 44078–44082.
26. Zhang, L., Zhang, Z., Long, F. & Lee, E. Y. (1996). Tyrosine-272 is involved in the inhibition of protein phosphatase-1 by multiple toxins. *Biochemistry*, **35**, 1606–1611.
27. Burgi, H. B., Dunitz, J. D. & Shefter, E. (1973). Geometrical reaction coordinates. 2. Nucleophilic addition to a carbonyl group. *J. Am. Chem. Soc.* **95**, 5065–5067.
28. Drahl, C., Cravatt, B. F. & Sorensen, E. J. (2005). Protein-reactive natural products. *Angew Chem. Int. Ed. Engl.* **44**, 5788–5809.
29. Maynes, J. T., Perreault, K. R., Cherney, M. M., Luu, H. A., James, M. N. G. & Holmes, C. F. B. (2004). Crystal structure and mutagenesis of a protein phosphatase-1: calcineurin hybrid elucidate the role of the beta 12-beta 13 loop in inhibitor binding. *J. Biol. Chem.* **279**, 43198–43206.
30. Moorhead, G., MacKintosh, R. W., Morrice, N., Gallagher, T. & MacKintosh, C. (1994). Purification of type 1 protein (serine/threonine) phosphatases by microcystin-Sepharose affinity chromatography. *FEBS Letters*, **356**, 46–50.
31. Kondo, F., Ikai, Y., Oka, H., Okumura, M., Ishikawa, N., Harada, K. *et al*. (1992). Formation, characterization, and toxicity of the glutathione and cysteine conjugates of toxic heptapeptide microcystins. *Chem. Res. Toxicol.* **5**, 591–596.
32. Williams, D. E., Craig, M., Dawe, S. C., Kent, M. L., Holmes, C. F. B. & Andersen, R. J. (1997). Evidence for a covalently bound form of microcystin-LR in salmon liver and dungeness crab larvae. *Chem. Res. Toxicol.* **10**, 1293.
33. Williams, D. E., Dawe, S. C., Kent, M. L., Andersen, R. J., Craig, M. & Holmes, C. F. (1997). Bioaccumulation and clearance of microcystins from salt water mussels, *Mytilus edulis*, and *in vivo* evidence for covalently bound microcystins in mussel tissues. *Toxicon*, **35**, 1617–1625.
34. Fischer, W. J., Hitzfeld, B. C., Tencalla, F., Eriksson, J. E., Mikhailov, A. & Dietrich, D. R. (2000). Microcystin-LR toxicodynamics, induced pathology, and immunohistochemical localization in livers of blue-green algae exposed rainbow trout (oncorhynchus mykiss). *Toxicol. Sci.* **54**, 365–373.
35. Hastie, C. J., Borthwick, E. B., Morrison, L. F., Codd, G. A. & Cohen, P. T. (2005). Inhibition of several protein phosphatases by a non-covalently interacting microcystin and a novel cyanobacterial peptide, nostocyclin. *Biochim. Biophys. Acta*, **18**, 18.
36. Powell, H. R. (1999). The Rossmann Fourier autoindexing algorithm in MOSFLM. *Acta Crystallog. sect. D*, **55**, 1690–1695.
37. Bailey, S. (1994). The CCP4 suite—programs for protein crystallography. *Acta Crystallog. sect. D*, **50**, 760–763.
38. Navaza, J. & Saludjian, P. (1997). AMoRe: an automated molecular replacement program package *Macromolecular Crystallography,* Part A, vol. 276 pp. 581–594.
39. McRee, D. E. (1999). XtalView Xfit—a versatile program for manipulating atomic coordinates and electron density. *J. Struct. Biol.* **125**, 156–165.
40. Murshudov, G. N., Vagin, A. A. & Dodson, E. J. (1997). Refinement of macromolecular structures by the maximum-likelihood method. *Acta Crystallog. sect. D*, **53**, 240–255.
41. Laskowski, R. A., Moss, D. S. & Thornton, J. M. (1993). Main-chain bond lengths and bond angles in protein structures. *J. Mol. Biol.* **231**, 1049–1067.
42. Hooft, R. W., Vriend, G., Sander, C. & Abola, E. E. (1996). Errors in protein structures. *Nature*, **381**, 272.

***Edited by M. Guss***

*(Received 1 September 2005; received in revised form 6 November 2005; accepted 7 November 2005)*
Available online 22 November 2005